



Preparation of polyaniline/diazonium salt/TiO₂ nanotube arrays as supercapacitor electrode by electrochemical grafting and deposition

Qinlei Chen¹ · Zhengbin Xia¹ · Yanhong Zhang¹ · Shumin Wang¹

Received: 2 June 2019 / Revised: 8 September 2019 / Accepted: 9 September 2019 / Published online: 20 November 2019
© Springer-Verlag GmbH Germany, part of Springer Nature 2019

Abstract

Polyaniline/diazonium salt/TiO₂ nanotube arrays (PANI/DZ/TiO₂ NAs), as a supercapacitor electrode material, are fabricated by two-step anodic oxidation of titanium foils, electrochemical grafting and reduction of diazonium salts, and electrochemical deposition of polyaniline. Surface morphology, crystallization, and chemical compositions of nanocomposites are characterized by SEM, EDX, XRD, and Raman. Electrochemical tests indicate that PANI/DZ/TiO₂ NAs have excellent capacitance of 1108.5 F g⁻¹ when the current density is 0.6 A g⁻¹. With the current density increasing 20 times to 12 A g⁻¹, the capacitance remains about 77.5%, demonstrating its good rate performance. Moreover, after 2000 charge–discharge cycles at 12 A g⁻¹, the capacitance retains 83.7% of the initial value, showing its good cycling stability.

Keywords Titanium dioxide nanotube arrays · Diazonium salts · Polyaniline · Electrochemical performance · Supercapacitor

Introduction

With the increase of resource and energy consumption and the enhancement of production capacity, the research of energy storage components with high specific capacitance, high conductivity, and long life has become an important issue in achieving sustainable development [1, 2]. In this condition, supercapacitors have received more and more attention and become one of the research hotspots in the field of electrochemistry [3, 4]. Electrode materials used in supercapacitors can be classified into inorganic materials (metal oxides [5], metal hydroxides [6], and carbon materials [7], etc) and organic materials (polyaniline [8], polythiophene [9], and polypyrrole [10], etc). Nanostructured electrodes have higher utilization efficiency than conventional electrodes, and the combination of organic and inorganic nanomaterials is the key to improving electrode performance [11, 12].

Recently, titanium dioxide nanotube arrays (TiO₂ NAs) having excellent aspect ratio, good mechanical stability, and

controllable size can be used as substrates composited with conductive polymer having high electrochemical activity, thereby obtaining nanocomposite electrodes that can be used in the field of supercapacitors [13–15]. Wang et al. fabricated high-performance polyaniline/bulk abundant Ti³⁺ self-doped TiO₂ nanotubes (PANI/MR-TiO₂ NAs) for supercapacitors by microwave-assisted self-doping and electrochemical deposition [16]. Although the specific capacitance of the composite electrode prepared by this method can reach 1084 F g⁻¹, the cycle stability is still not very satisfactory. The surface of the TiO₂ NAs is very smooth, and PANI accumulates on the surface of TiO₂ NAs by simple physical action, so the adhesion between PANI and TiO₂ NAs substrate is weak [16–18]. During the process of charging and discharging, PANI will expand and contract repeatedly, which will cause PANI to fall off the surface of TiO₂ NAs easily, thus showing poor cycling stability [19]. There are two ways to make the organic/inorganic nanocomposite more stable. The first way is direct surface grafting. The polymers with active end groups are directly introduced into the active sites on the surface of inorganic nanomaterials through chemical bonding [19–21]. The second way is connection by coupling agent. The coupling reaction occurs on the surface of the inorganic nanomaterial to form an initiation point of polymerization; then, the polymers are prepared by electrochemical polymerization and attached to the surface of inorganic nanomaterials [22, 23].

✉ Zhengbin Xia
cezhbxia@scut.edu.cn

¹ School of Chemistry and Chemical Engineering, South China University of Technology, Guangzhou 510641, Guangdong, China

Diazonium salts, as a new type of coupling agent, can be used for surface functionalization to attach polymers to the substrate surface [24]. The use of diazonium salts for surface modification was first introduced by Delamar et al. in 1992 [25]. Electrochemical reduction can be performed on the diazonium salt and its derivatives attached to the substrate surface to achieve surface functionalization [24, 26, 27]. Aryl diazonium salts composed of anions, aryl groups, azide groups, and other functional groups are widely used in the field. During the grafting process, the azide groups leave in the form of nitrogen while the aryl moieties form covalent bonds with the substrate surface [28, 29]. Through the grafting process, not only the target groups can be directly introduced into the surface of substrate, but also subsequent reactions can be carried out on the grafted groups to obtain a surface with different chemical properties. And the functional groups can be used as graft initiators for subsequent polymerization routes or binding sites for preformed polymers [24, 27, 30].

In this paper, TiO_2 NAs are firstly prepared by electrochemical anodic oxidation of titanium foils; then, TiO_2 NAs are modified by the diazonium salt through electrochemical method. One end of the diazonium salt is tightly linked to

TiO_2 NAs through the covalent bond after grafting process, and the other end is electrochemically reduced to an aniline group, which provides an active site for subsequent electrochemical polymerization of PANI. Finally, PANI is electropolymerized and deposited on modified electrodes to obtain PANI/DZ/ TiO_2 NAs. The mechanism of modification by 4-nitrobenzene diazonium tetrafluoroborate and the preparation procedure are shown in Fig. 1.

Experimental section

Materials synthesis

Preparation of TiO_2 NAs

Briefly, titanium foils (purity 99.9%, size $13 \times 10 \times 1$ mm) were used as raw materials to prepare TiO_2 NAs samples by two-step anodization at room temperature [31]. During pre-treatment before anodizing, the titanium foils need to be ground smooth with 500 and 1200 sandpapers and rinsed in a 2 wt% HF solution for about 6 s. The experimental system

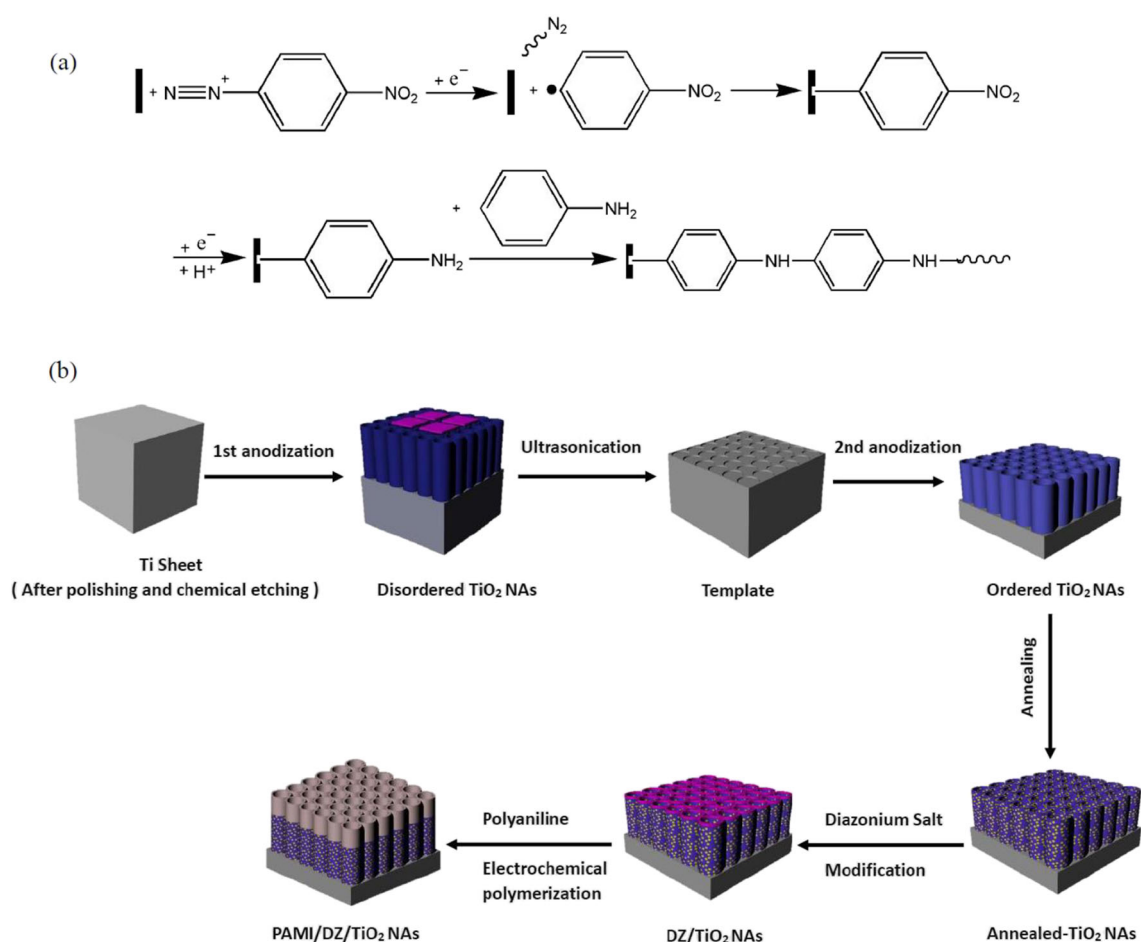


Fig. 1 a Mechanism of modification by 4-nitrobenzene diazonium tetrafluoroborate. (b) Preparation procedure of PANI/DZ/ TiO_2 NAs

used in the electrochemical process is a two-electrode cell that uses direct current as the power source and a Pt foil as the counter electrode. The first anodization was carried out in ethylene glycol electrolyte (0.5 wt% NH_4F and 2 vol% deionized water) at 60 V for 2 h. Next, the oxidized sample was subjected to remove the oxide films by ultrasonic treatment in deionized water to obtain titanium foils having base patterns. Afterwards, the second anodization of the well-patterned titanium foils was carried out in another ethylene glycol electrolyte (0.5 wt NH_4F 2 vol% deionized water and 0.5 wt% H_3PO_4) at 60 V for 30 min. Finally, the two-step oxidized TiO_2 NAs were calcined in air at 450 °C for 2 h to transform the amorphous TiO_2 NAs into anatase.

Fabrication of DZ/ TiO_2 NAs

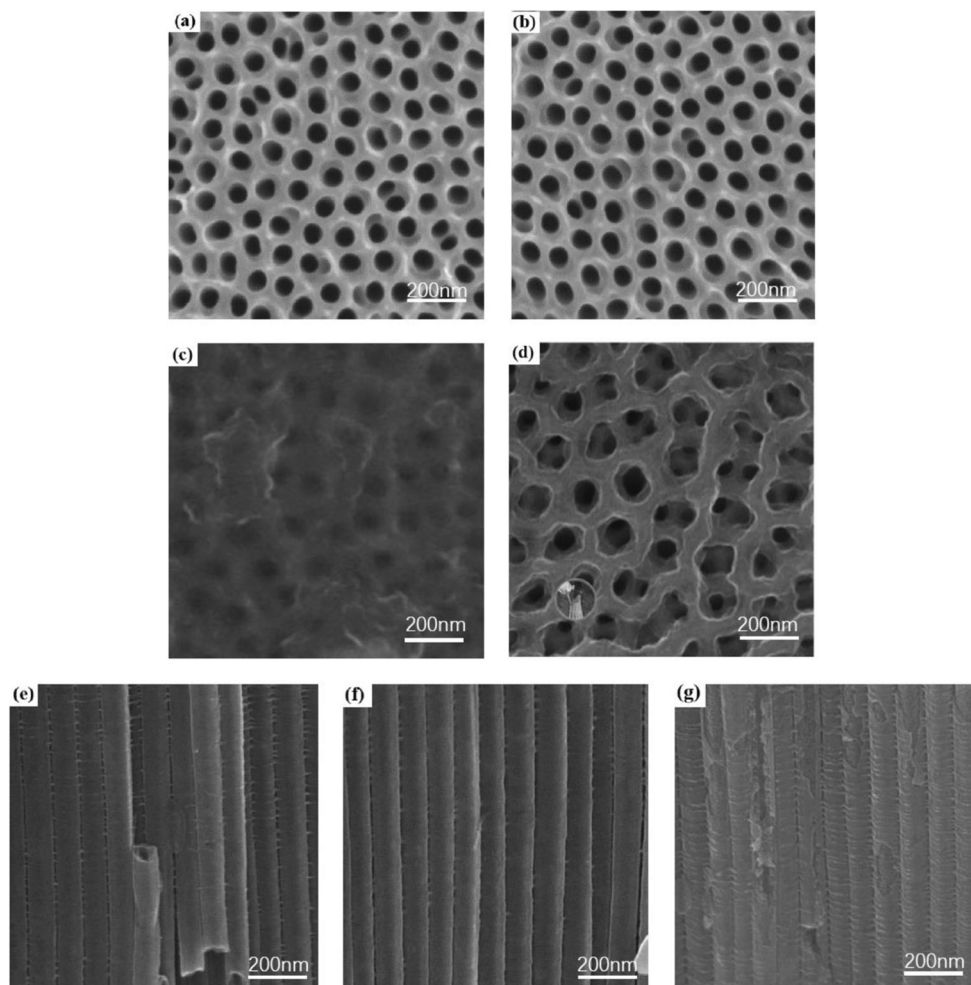
The surface modification of TiO_2 NAs with the diazonium salt was carried out by cyclic voltammetry (CV) at room temperature in a three-electrode cell (Pt foil as a counter electrode, saturated calomel electrode (SCE) as a reference electrode, TiO_2 NAs as a working electrode). The first step was

completed in acetonitrile electrolyte (2 mM 4-nitrobenzenediazonium tetrafluoroborate and 0.2 M TBAPF6) with a scanning rate of 10 mV s^{-1} ranging from 0.4 to -0.7 V for 2 cycles. The reduction of the diazonium salt was carried out in a water–ethanol electrolyte (90:10 vol%, 0.1 M KCl) with a scanning rate of 50 mV s^{-1} ranging from -1.2 to 0.2 V for 1 cycles.

Fabrication of PANI/DZ/ TiO_2 NAs

PANI/DZ/ TiO_2 NAs were prepared by electrochemical polymerization in the same three-electrode cell as “Fabrication of DZ/ TiO_2 NAs.” Firstly, the DZ/ TiO_2 NAs needed to be immersed in acetone solutions (0.5 M H_2SO_4 and 0.2 M aniline) for 12 h. After rinsing with ethanol and deionized water, the polymerization process was carried out by CV in an aqueous solution (0.5 M H_2SO_4 and 0.1 M aniline) with a scanning rate of 25 mV s^{-1} ranging from -0.4 to 1.3 V for 5 cycles. After washing the PANI/DZ/ TiO_2 NAs electrode with deionized water, dry it naturally in the air.

Fig. 2 Top and cross-sectional SEM images of **a, e** pristine TiO_2 NAs, **b** DZ/ TiO_2 NAs, **c, f** PANI/ TiO_2 NAs, and **d, g** PANI/DZ/ TiO_2 NAs



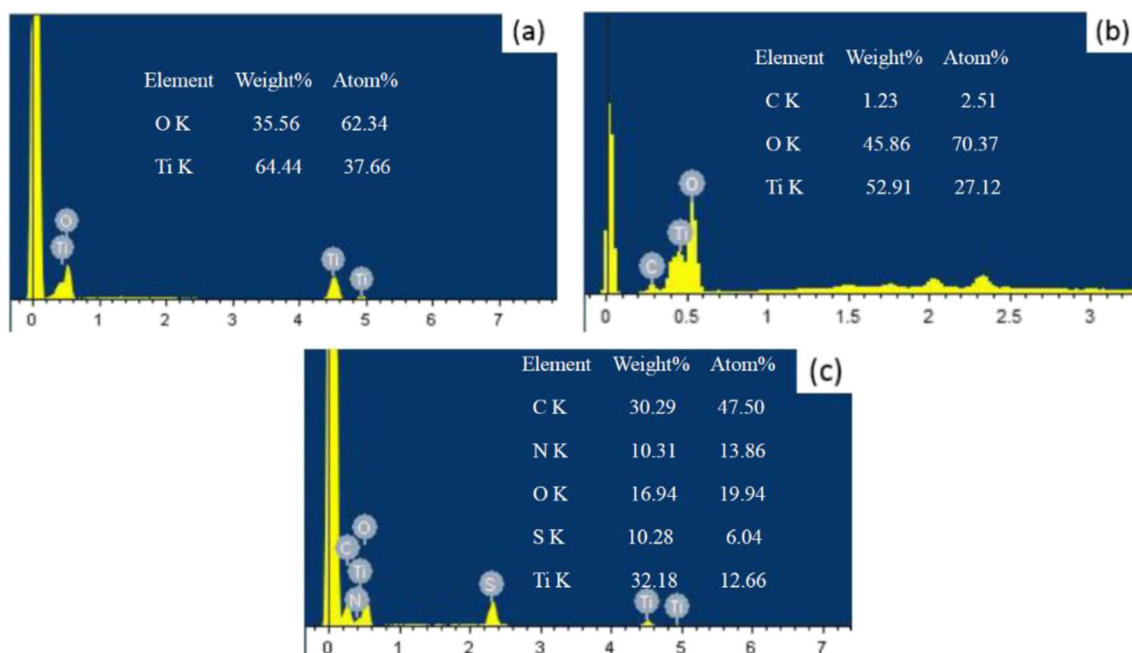


Fig. 3 EDX spectrums of **a** TiO₂ NAs, **b** DZ/TiO₂ NAs, and **c** PANI/DZ/TiO₂ NAs

For comparison, TiO₂ NAs was subjected to the same immersion and electrochemical polymerization deposition processes to prepare PANI/TiO₂ NAs.

cycle stability of PANI/DZ/TiO₂ NAs samples was measured by GCD at 12.0 A g⁻¹ and the voltage varied between 0 and 0.65 V up to 2000 times.

Electrochemical measurements

The measurements of electrochemical properties were taken on an electrochemical workstation (CHI608E, USA) in an aqueous solution (1.0 M HCl) in the same three-electrode cell as “Fabrication of DZ/TiO₂ NAs.” The test methods included cyclic voltammetry (CV) and galvanostatic charge–discharge (GCD). The scanning range of CV was -0.2 to 1.0 V, the current density of GCD ranged from 0.6 to 1.2 A g⁻¹. The

Characterization

The microtopography of electrodes was observed by a field emission scanning electron microscopy (FE-SEM, Hitachi SU-8220, Japan) at an acceleration voltage of 10 KV. The crystallization and chemical compositions were measured by X-ray diffraction (XRD) and Raman spectrums. XRD spectrums were recorded by an X-ray diffractometer (Bruker D8

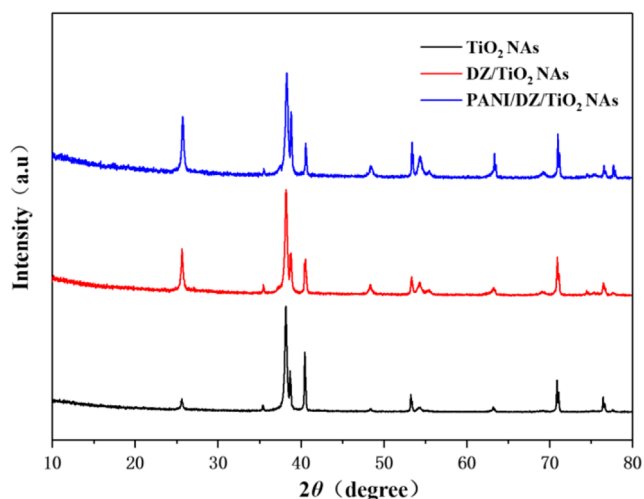


Fig. 4 XRD spectrums of TiO₂ NAs, DZ/TiO₂ NAs, and PANI/DZ/TiO₂ NAs

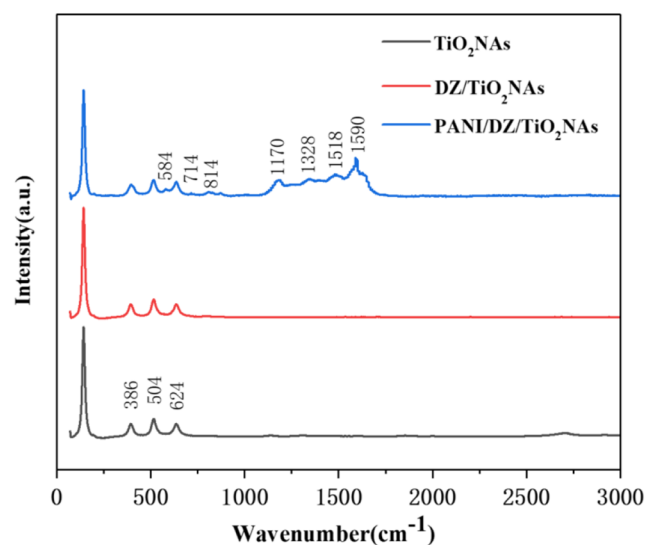


Fig. 5 Raman spectrums of TiO₂ NAs, DZ/TiO₂ NAs, and PANI/DZ/TiO₂ NAs

ADVANCE, Germany) at 40 KV and 40 mA using Cu K α radiation. The Raman spectrums were obtained by a Raman spectrometer (HORIBA Jobin Yvon LabRAM Aramis, France) and the incident power of line was 10.4 mW and the excitation wavelength was 532 nm. The weight of electrodes was weighed by a precision electronic balance (Mettler Toledo, MX5).

Results and discussion

Surface microtopography

Figure 2 shows the top and cross-sectional SEM images of pristine TiO₂ NAs, DZ/TiO₂ NAs, PANI/TiO₂ NAs, and PANI/DZ/TiO₂ NAs. It can be seen that, by the anodization process, the highly ordered and well-separated TiO₂ NAs with an interior diameter of about 100 nm. Figure 2 b shows the surface morphology of DZ/TiO₂ NAs with no significant change compared with TiO₂ NAs in Fig. 2a, because the graft layer is a monolayer. The structure of PANI/TiO₂ NAs is shown in Fig. 2c, f, the top of TiO₂ NAs is coated and blocked by disordered PANI, the nanotube wall is also covered by a thin layer of PANI, and the original structure of TiO₂ NAs is not destroyed compared with Fig. 2e. Because the surface of TiO₂ NAs is very smooth, PANI accumulates on the surface of nanotube by a simple physical action. As shown in Figs. 2d, g, with diazonium salts as connecting agents, PANI/DZ/TiO₂ NAs exhibits the same regular surface as the original TiO₂ NAs. The top and cross-sectional of PANI/DZ/TiO₂ NAs are rough, the top of the nanotubes is not blocked by PANI, and the sample maintains a highly ordered nanotube morphology, because PANI grows longitudinally along the surface of DZ/TiO₂ NAs. This structure is significant to the properties of the composite materials and provides a fast channel for ion diffusion and electronic transmission, thus greatly improving the electrochemical performance of composite electrode materials [15].

The compositions of TiO₂ NAs, DZ/TiO₂ NAs, and PANI/DZ/TiO₂ NAs can be analyzed by energy-dispersive X-ray analyzer (EDX) installed in the SEM device. As shown in Fig. 3b, the DZ/TiO₂ NAs contains O, Ti, and C elements, indicating the existence of the diazonium salt on the nanotubes, because of the additional C element compared with TiO₂ NAs (Fig. 3a). However, no N element is detected, which may be due to the content of N element being too low to be detected or the characteristic peak is covered by O element. In Fig. 3c, compared with DZ/TiO₂ NAs, the content of

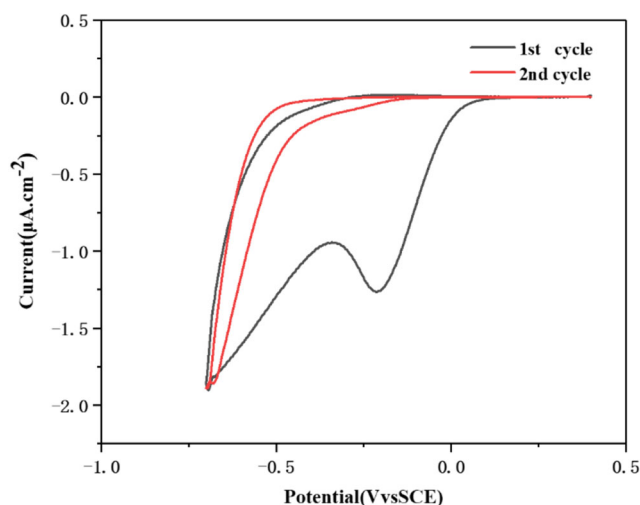


Fig. 6 Two consecutive CV profiles of grafting the diazonium salt with a scanning rate of 10 mV s⁻¹ and a potential range of 0.4 to -0.7 V (vs. SCE)

C element in PANI/DZ/TiO₂ NAs is greatly increased and N element is detected, indicating that PANI has been deposited on DZ/TiO₂ NAs. In addition, PANI/DZ/TiO₂ NAs also contain the S element, because the electrochemical polymerization process was carried out in the aqueous solution containing sulfuric acid.

Crystallization and chemical compositions

The XRD spectrums of TiO₂ NAs, DZ/TiO₂ NAs, and PANI/DZ/TiO₂ NAs are shown in Fig. 4. The characteristic peaks (25.3, 37.8, 47.9, 54.4, and 55.5 cm⁻¹) corresponding to anatase TiO₂ (JCPDS file 71-1167) and other characteristic peaks corresponding to Ti (JCPDS file 05-0682) indicate that annealing can convert amorphous TiO₂ NAs into anatase and subsequent reactions do not affect the anatase crystal form [32, 33].

However, compared with TiO₂ NAs, no additional characteristic peaks of the diazonium salt and PANI are found in the XRD patterns of DZ/TiO₂ NAs and PANI/DZ/TiO₂ NAs, which may be due to the content of the diazonium salt being too low to be detected and PANI is amorphous or the introduction of the TiO₂ hampers the crystallization of the PANI molecular chains [34, 35].

Raman spectrums of TiO₂ NAs, DZ/TiO₂ NAs, and PANI/DZ/TiO₂ NAs are presented in Fig. 5. In all samples, there are four anatase peaks at about 143, 386, 504, and 624 cm⁻¹, consistent with the result of XRD [36]. Compared with TiO₂ NAs, DZ/TiO₂ NAs has no obvious additional

Table 1 The weight of TiO₂ NAs, DZ/TiO₂ NAs, and PANI/DZ/TiO₂ NAs

Samples	TiO ₂ NAs	DZ/TiO ₂ NAs	PANI/DZ/TiO ₂ NAs	PANI/TiO ₂ NAs
Weight (mg)	4.346 ± 0.001	4.365 ± 0.001	5.942 ± 0.001	5.771 ± 0.001

characteristic peaks, because the content of the diazonium salt monolayer is too low to be detected. PANI/DZ/TiO₂ NAs have the characteristic peaks of PANI. The characteristic peaks located in 1518 cm⁻¹ and 1590 cm⁻¹ are caused by the C=N expansion vibration of the quinone unit and the C=C expansion vibration in the quinonoid ring, respectively, while the two characteristic peaks in 1170 and 814 cm⁻¹ are due to the C–N vibrations of the polarized carrier. The C–H vibrational peaks of the benzene ring are located at 814 and 1170 cm⁻¹. The other three peaks at 713, 588, and 294 cm⁻¹ are also characteristic peaks of PANI according to other literatures [35, 37]. Raman spectrums strongly confirm that PANI has been successfully deposited on TiO₂ NAs.

The weight of TiO₂ NAs, DZ/TiO₂ NAs, and PANI/DZ/TiO₂ NAs are weighed by a precision electronic balance, and the results are shown in Table 1. The mass of DZ/TiO₂ NAs is larger than TiO₂ NAs, indicating the existence of the diazonium salt. And the mass of PANI/DZ/TiO₂ NAs is significantly larger than that of DZ/TiO₂ NAs, which is the result of PANI deposition.

Electrochemical performance

CV is commonly applied to test and characterize the capacitance performance of electrodes. Capacitance values under

test conditions can be obtained by calculating the cycle curves using the following formulas [8]:

$$C_s = (I \Delta V) / (\nu \times S \times V) \quad (1)$$

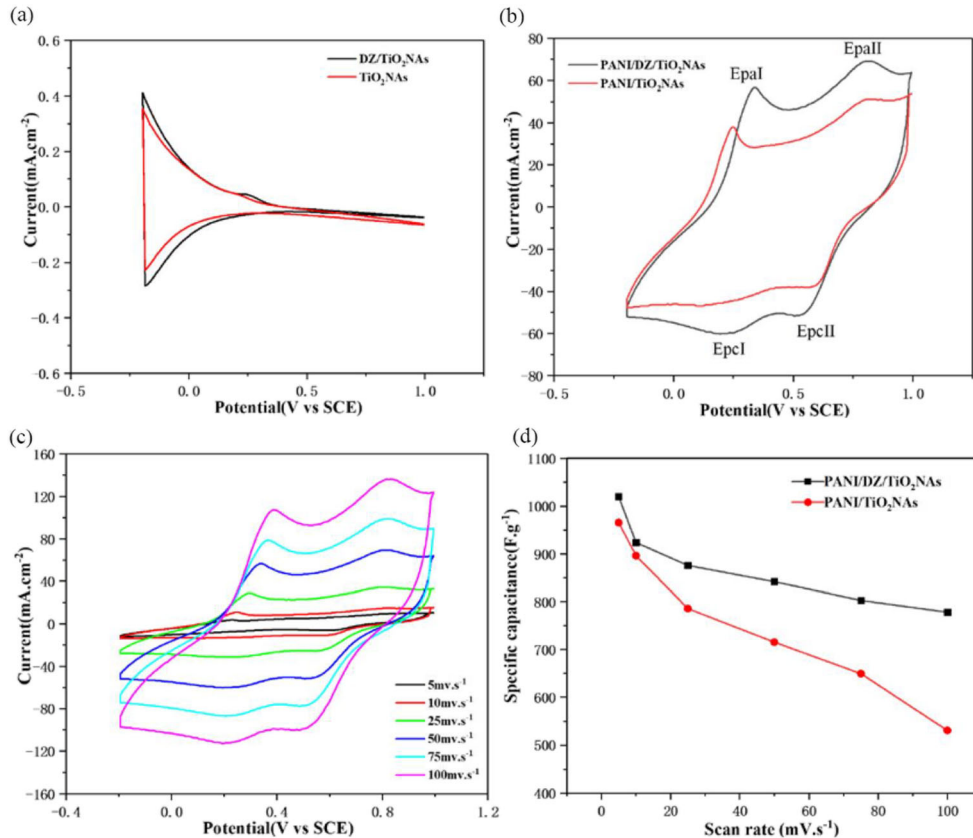
$$C_m = (I \Delta V) / (\nu \times m \times V) \quad (2)$$

where C_s is the unit-area capacitance (mF cm⁻²), C_m the unit-mass capacitance (F g⁻¹), I the current intensity (A), ν the scanning rate (mV s⁻¹), V the electric potential (V), S the surface area of a measured sample (cm²), and m the mass of active substances on the measured sample (g).

Figure 6 presents the CV profiles of grafting the diazonium salt onto TiO₂ NAs in an acetonitrile solution (2 mM 4-nitrobenzenediazonium tetrafluoroborate and 0.2 M TBAPF6) with a scanning rate of 10 mV s⁻¹ between 0.4 and -0.7 V. The irreversible cathode peak appears at about -0.2 V in the first curve indicating that the diazonium salt is reduced. On the second cycle curve, the cathode peak disappears because the organic layer has blocked the surface and hindered the continuous reactions, so the graft layer is a monolayer [38, 39]. This result confirms that diazonium salt has been successfully grafted onto the surface of TiO₂ NAs and the graft layer is a monolayer [40, 41].

Figure 7 a shows the CV profiles of TiO₂ NAs and DZ/TiO₂ NAs with a scanning rate of 50 mV s⁻¹ and a potential range of -0.2 to 1.0 V (vs. SCE), CV profiles b of PANI/TiO₂ NAs and PANI/DZ/TiO₂ NAs with a scanning rate of 50 mV s⁻¹ and a potential range of -0.2 to 1.0 V (vs. SCE), CV profiles c of PANI/DZ/TiO₂ NAs at different scanning rate from 5 to 100 mV s⁻¹ with a potential range of -0.2 to 1.0 V (vs. SCE), and the specific capacitance d of PANI/TiO₂ NAs and PANI/DZ/TiO₂ NAs in terms of the scanning rate

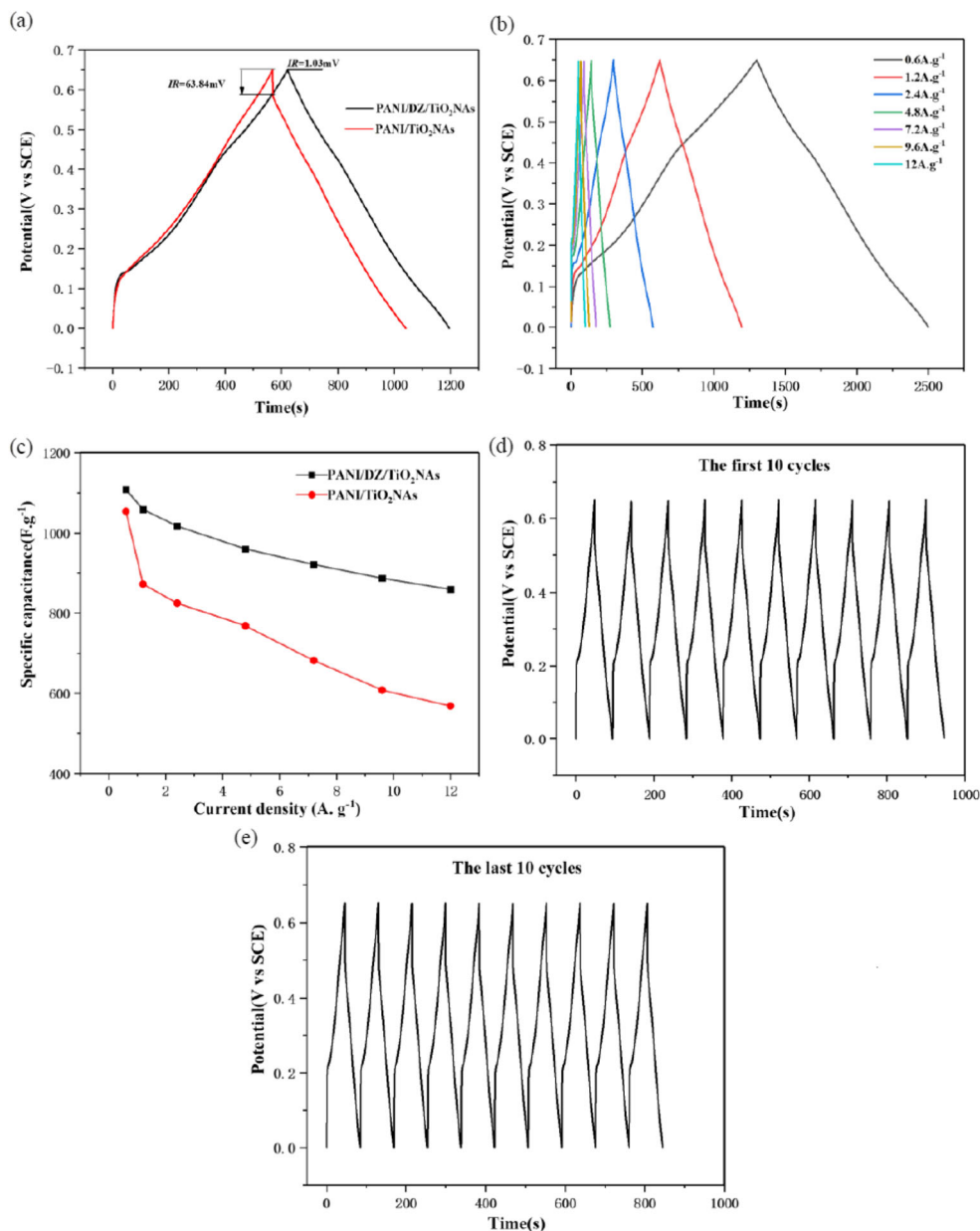
Fig. 7 CV profiles **a** of TiO₂ NAs and DZ/TiO₂ NAs with a scanning rate of 50 mV s⁻¹ and a potential range of -0.2 to 1.0 V (vs. SCE), CV profiles **b** of PANI/TiO₂ NAs and PANI/DZ/TiO₂ NAs with a scanning rate of 50 mV s⁻¹ and a potential range of -0.2 to 1.0 V (vs. SCE), CV profiles **c** of PANI/DZ/TiO₂ NAs at different scanning rate from 5 to 100 mV s⁻¹ with a potential range of -0.2 to 1.0 V (vs. SCE), and the specific capacitance **d** of PANI/TiO₂ NAs and PANI/DZ/TiO₂ NAs in terms of the scanning rate



aqueous solution. The CV profiles of the two samples are similar and exhibit similar pseudocapacitive characteristic properties [8]. The electrochemical properties of TiO₂ NAs are not significantly affected by the use of the diazonium salt alone. Figure 7 b shows the CV profiles of PANI/TiO₂ NAs and PANI/DZ/TiO₂ NAs. Two pairs of redox peaks are found in PANI/TiO₂ NAs and PANI/DZ/TiO₂ NAs, indicating the pseudocapacitive characteristics of PANI [42]. The first pair of redox peaks (EpcI/EpaI) at about 0.205/0.335 V is due to the transition of PANI between leucoemeraldine and emeraldine states, and another pair of redox peaks (EpcII/EpaII) at approximately 0.535/0.815 V is due to the transition between emeraldine and pernigraniline states. Compared with PANI/TiO₂ NAs, the area of CV curve of PANI/DZ/TiO₂

NAs is larger, and after calculation, PANI/DZ/TiO₂ NAs have a specific capacitance of 841.8 F g⁻¹ more than that of PANI/TiO₂ NAs (715.5 F g⁻¹). Because the diazonium salt acts as a bridge between PANI and TiO₂ NAs, one end of the diazonium salt is connected to TiO₂ NAs through the covalent bond, and the other end can provide an active site for subsequent reactions. Thus, the morphology and structure of PANI/DZ/TiO₂ NAs are more orderly, resulting in higher specific capacitance. From the CV curves shown in Fig. 7c, it can be seen that PANI/DZ/TiO₂ NAs have similar redox peaks at different scanning rates. The first pair of redox peaks is caused by a redox reaction inside the electrode, and the second pair is caused by redox reaction at the surface or near the surface. And the redox peaks are shifted by polarization at different

Fig. 8 GCD profiles **a** of PANI/TiO₂ NAs and PANI/DZ/TiO₂ NAs at the current density of 1.2 A g⁻¹, GCD profiles **b** of PANI/DZ/TiO₂ NAs at different current density from 0.6 A g⁻¹ to 12 A g⁻¹, the specific capacitance **c** of PANI/TiO₂ NAs and PANI/DZ/TiO₂ NAs in terms of current density, the first **d** 10 cycles and the **e** last 10 cycles GCD profiles of PANI/DZ/TiO₂ NAs for 2000 cycles at the current density of 12 A g⁻¹



scanning rates, the anode peaks move positively, and the cathode peaks move negatively, which indicates the occurrence of irreversible redox reaction [19]. The specific capacitance of PANI/DZ/TiO₂ NAs and PANI/TiO₂ NAs calculated by CV profiles at different scanning rates are shown in Fig. 7d. With the scanning rate increasing from 5 to 100 mV s⁻¹, the specific capacitance of PANI/DZ/TiO₂ NAs decreased from 1020.1 to 778.3 F g⁻¹, retaining 76.3% of the initial capacitance, while the value of PANI/TiO₂ NAs is only 54.9%, indicating PANI/DZ/TiO₂ NAs have high specific capacitance, good stability, and high rate performance, because the diazonium salt makes TiO₂ NAs and PANI connect closely by converting physical deposition into chemical covalent grafting [23].

High power performance is a key issue for supercapacitor applications. The capacitance can be calculated from GCD profiles using the following formulas [18]:

$$C_s = (I \times \Delta t) / (S \times \Delta V) \quad (3)$$

$$C_m = (I \times \Delta t) / (m \times \Delta V) \quad (4)$$

where C_s is the unit-area capacitance (mF cm⁻²), C_m the unit-mass capacitance (F g⁻¹), I the constant current intensity (A), Δt the discharge duration (s), ΔV the potential range (V), S the surface area of measured sample (cm²), and m the mass of active substances on the measured sample (g).

Figure 8 a shows the GCD profiles of PANI/TiO₂ NAs and PANI/DZ/TiO₂ NAs. At the same current density of 1.2 A g⁻¹, the specific capacitance values of PANI/DZ/TiO₂ NAs and PANI/TiO₂ NAs are 1058.8 F g⁻¹ and 872.3 F g⁻¹, respectively. The voltage drop (IR) in the positive branch is caused by the total resistance along the electric circuit, including the resistance of a working electrode material and electrolyte solution, so the IR drop of both electrodes is about 130 mV. And the IR drop in the negative branch is caused by internal resistance of the electrode material, so the IR drop of PANI/DZ/

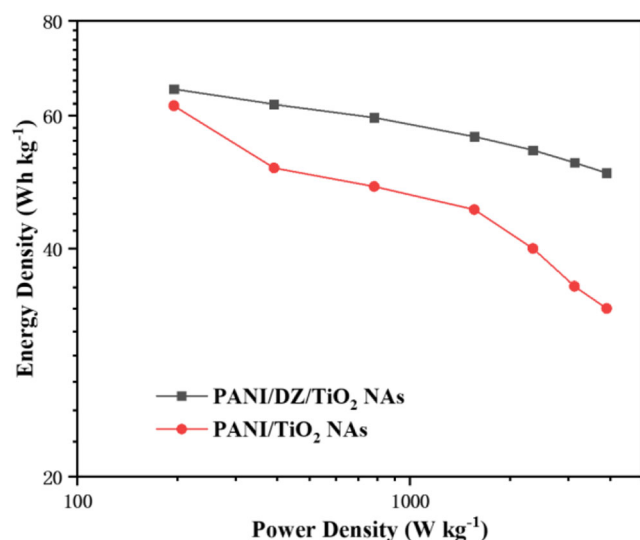


Fig. 9 Ragone plots of PANI/DZ/TiO₂ NAs and PANI/TiO₂ NAs

TiO₂ NAs is only 1.03 mV, slightly smaller than that of PANI/TiO₂ NAs (63.84 mV), indicating that PANI/DZ/TiO₂ NAs has higher specific capacitance, smaller internal resistance, and better charge transfer capability after being modified by the diazonium salt. In addition, it can be seen that the faradaic reaction occurred in both samples because the charge–discharge curves are non-linear [43].

The GCD profiles of PANI/DZ/TiO₂ NAs between 0 and 0.65 V at different current densities are shown in Fig. 8b. As shown in Fig. 8c, with the current density increasing 20 times to 12 A g⁻¹, the specific capacitance of PANI/DZ/TiO₂ NAs and PANI/TiO₂ NAs decreases. The drop is caused by the kinetic limitation of the pseudocapacitance redox reaction of PANI. With the increase of current density, the charging and discharging time become shorter, and the electrochemical reaction rate lags behind the electron transport, resulting in the decrease of pseudocapacitance [15]. At the same time, during the charging and discharging cycles, the doping or de-doping of H⁺ in the PANI chains leads to the expansion, shrinkage, and drop of polymer materials, resulting in the reduction of electrode capacitance [44]. The value of specific capacitance of PANI/DZ/TiO₂ NAs drops from 1108.5 to 859.0 F g⁻¹ (Fig. 8c), remaining 77.5%, more than that of PANI/TiO₂ NAs (54.0%), again indicating the better rate performance of PANI/DZ/TiO₂ NAs. To investigate the cycling stability, Figs. 8d, e respectively show the GCD curves of the first 10 cycles and the last 10 cycles of PANI/DZ/TiO₂ NAs during the 2000 charge–discharge process, when the voltage range is 0–0.65 V and the current intensity is 12 A g⁻¹. It can be observed that the IR drop increases with the cycling time and is more pronounced in the negative branch than in the positive branch as the cycle time increases, because the conductivity of the electrode is more affected than the ion diffusion process. After 2000 cycles of charge and discharge, the capacitance value of PANI/DZ/TiO₂ NAs is calculated to be 719.1 F g⁻¹, which is 83.7% of the initial value and shows excellent cycling stability. Excellent cycle stability is attributed to the highly ordered and well-separated nanocomposite structure. After surface modification by the diazonium salt, PANI can uniformly connect to the surface of TiO₂ NAs, so that the nanotubes can support PANI effectively and avoid structural collapse [17, 45].

The specific energy density (E) and power density (P) of samples can be calculated from GCD profiles using the following formulas [43]:

$$E = (I \times \Delta V \times \Delta t) / 2m \quad (5)$$

$$P = (I \times \Delta V) / 2m \quad (6)$$

where E is the specific energy density (Wh Kg⁻¹), P the power density (W Kg⁻¹), I the constant current intensity (A), Δt the discharge duration (s), ΔV the potential range (V), and m the mass of active substances on the measured sample (Kg).

As shown in Fig. 9, at the same power density, the energy density of PANI/DZ/TiO₂ NAs is higher than that of PANI/TiO₂ NAs. At the current density of 1.2 A g⁻¹, when the power density is 390 W Kg⁻¹, the energy density of PANI/DZ/TiO₂ NAs and PANI/TiO₂ NAs are 62.13 Wh Kg⁻¹ and 51.19 Wh Kg⁻¹, respectively. PANI/DZ/TiO₂ NAs has better energy storage capability and can be used in the field of supercapacitors, because the organic polymer and the inorganic electrode substrate are connected more closely.

Conclusions

In summary, the PANI/DZ/TiO₂ NAs nanocomposite, with PANI growing along the surface of nanotubes, can be obtained via three steps: anodization, surface modification, and electrochemical polymerization. After surface modification of the diazonium salt, PANI/DZ/TiO₂ NAs have higher specific capacitance and conductivity, better electron transport capability cycling stability, and energy storage capability than PANI/TiO₂ NAs. This result is attributed to the highly ordered structure of PANI/DZ/TiO₂ NAs, which increases the effective specific surface area of the interfacial reaction, and provides fast and efficient channels for ion diffusion and electron transport. Otherwise, PANI and TiO₂ NAs are covalently linked by the diazonium salt and PANI can be supported by TiO₂ NAs effectively, which enhances the stability of the nanocomposite greatly.

References

- Simon P, Gogotsi Y, Dunn B (2014) Where do batteries end and supercapacitors begin? *Science* 343(6176):1210–1211
- Hu ZK, Zu L, Jiang YH, Lian HQ, Liu Y, Li ZZ, Chen F, Wang XD, Cui XG (2015) High specific capacitance of polyaniline/mesoporous manganese dioxide composite using KI-H₂SO₄ electrolyte. *Polymers* 7(10):1939–1953
- Stoller MD, Park SJ, Zhu YW, An JH, Ruoff RS (2008) Graphene-based ultracapacitors. *Nano Lett* 8(10):3498–3502
- Li ZH, Li LQ, Li ZP, Liao HY, Zhang HY (2016) Ultrathin carbon gauze for high-rate supercapacitor. *Electrochim Acta* 222:990–998
- Yu GH, Hu LB, Liu N, Wang HL, Vosgueritchian M, Yang Y, Cui Y, Bao ZN (2015) Enhancing the supercapacitor performance of graphene/MnO₂ nanostructured electrodes by conductive wrapping. *Nano Lett* 11:4438–4442
- Qi YH, Liu YF, Zhu R, Wang QL, Luo YL, Zhu CF, Lyu YN (2019) Rapid synthesis of Ni(OH)₂/graphene nanosheets and NiO@Ni(OH)₂/graphene nanosheets for supercapacitor applications. *New J Chem* 43(7):3091–3098
- Yan Z, Shi TL, Huang YY, Cheng SY, Liao GL, Tang ZR (2018) One-step synthesis of porous carbon derived from starch for all-carbon binder-free high-rate supercapacitor. *Electrochim Acta* 269:676–685
- Shao Z, Li HJ, Li MJ, Li CP, Qu CQ, Yang BH (2015) Fabrication of polyaniline nanowire/TiO₂ nanotube array electrode for supercapacitors. *Energy* 87:578–585
- Zhang HQ, Hu LW, Tu JG, Jiao SQ (2014) Electrochemically assembling of polythiophene film in ionic liquids (ILs) microemulsions and its application in an electrochemical capacitor. *Electrochim Acta* 120:122–127
- Sharma RK, Rastogi AC, Desu SB (2008) Pulse polymerized polypyrrole electrodes for high energy density electrochemical supercapacitor. *Electrochem Commun* 10(2):268–272
- He Y, Du SS, Li HL, Cheng QL, Pavlinek V, Saha P (2016) MnO₂/polyaniline hybrid nanostructures on carbon cloth for supercapacitor electrodes. *J Solid State Electrochem* 20(5):1459–1467
- Zang XB, Li X, Zhu M, Li XM, Zhen Z, He YJ, Wang KL, Wei JQ, Kang FY, Zhu HW (2015) Graphene/polyaniline woven fabric composite films as flexible supercapacitor electrodes. *Nanoscale* 7(16):7318–7322
- Li Q, Xia ZB, Wang SM, Zhang YJ, Zhang YH (2017) The preparation and characterization of electrochemical reduced TiO₂ nanotubes/polypyrrole as supercapacitor electrode material. *J Solid State Electrochem* 21(8):2177–2184
- Lee KY, Mazare A, Schmuki P (2014) One-dimensional titanium dioxide nanomaterials: nanotubes. *Chem Rev* 114(19):9385–9454
- Mujawar SH, Ambade SB, Battumur T, Ambade RB, Lee SH (2011) Electropolymerization of polyaniline on titanium oxide nanotubes for supercapacitor application. *Electrochim Acta* 56(12):4462–4466
- Wang SM, Xia ZB, Li Q, Zhang YH (2017) Fabrication of polyaniline/self-doped TiO₂ nanotubes hybrids as supercapacitor electrode by microwave-assisted chemical reduction and electrochemical deposition. *J Electrochem Soc* 164(13):D901–D907
- Palmas S, Mascia M, Vacca A, Llanos J, Mena E (2014) Analysis of photocurrent and capacitance of TiO₂ nanotube-polyaniline hybrid composites synthesized through electroreduction of an aryl diazonium salt. *RSC Adv* 4(46):23957–23965
- Xie KY, Li J, Lai YQ, Zhang ZA, Liu YX, Zhang GG, Huang HT (2011) Polyaniline nanowire array encapsulated in titania nanotubes as a superior electrode for supercapacitors. *Nanoscale* 3(5):2202–2207
- Xie S, Gan MY, Ma L, Li ZT, Yan J, Yin H, Shen XY, Xu FF, Zheng JY, Zhang J, Hu JL (2014) Synthesis of polyaniline-titania nanotube arrays hybrid composite via self-assembling and graft polymerization for supercapacitor application. *Electrochim Acta* 120:408–415
- Bousquet A, Awada H, Hioms RC, Dagron-Lartigau C, Billon L (2014) Conjugated-polymer grafting on inorganic and organic substrates: a new trend in organic electronic materials. *Prog Polym Sci* 39(11):1847–1877
- Higaki Y, Kobayashi M, Hirai T, Takahara A (2017) Direct polymer brush grafting to polymer fibers and films by surface-initiated polymerization. *Polym J* 50:101–108
- Assresahegn BD, Brousse T, Bélanger D (2015) Advances on the use of diazonium chemistry for functionalization of materials used in energy storage systems. *Carbon* 92:362–381
- Santos LM, Ghilane J, Fave C, Lacaze PC, Randriamahazaka H, Abrantes LM, Lacroix JC (2010) Electrografting polyaniline on carbon through the electroreduction of diazonium salts and the electrochemical polymerization of aniline. *J Phys Chem C* 112:16103–16109
- Mahouche-Chergui S, Gam-Derouich S, Mangeney C, Chehimi MM (2011) ChemInform abstract: aryl diazonium salts: a new class of coupling agents for bonding polymers, biomacromolecules and nanoparticles to surfaces. *Chem Soc Rev* 40(7):4143–4166
- Delamar M, Hitmi R, Pinson J, Saveant JM (1992) Covalent modification of carbon surfaces by grafting of functionalized aryl

- radicals produced from electrochemical reduction of diazonium salts. *J Am Chem Soc* 114(14):5883–5884
26. Allongue P, Delamar M, Desbat B, Fagebaume O, Hitmi R, Pinson J, Savéant JM (1997) Covalent modification of carbon surfaces by aryl radicals generated from the electrochemical reduction of diazonium salts. *J Am Chem Soc* 119:138–142
 27. Pinson J, Podvorica F (2005) Attachment of organic layers to conductive or semiconductive surfaces by reduction of diazonium salts. *Chem Soc Rev* 34(5):429–439
 28. Bélanger D, Pinson J (2011) Electrografting: a powerful method for surface modification. *Chem Soc Rev* 40(7):3995–4048
 29. Zeb G, Gaskell P, Le XT, Xiao X, Szkopek T, Cerruti M (2012) Decoration of graphitic surfaces with Sn nanoparticles through surface functionalization using diazonium chemistry. *Langmuir* 28(36):13042–13050
 30. Marwan J, Addou T, Bélanger D (2005) Functionalization of glassy carbon electrodes with metal-based species. *Chem Mater* 17(9):2395–2403
 31. Li H, Xing JH, Xia ZB, Chen JQ (2014) Preparation of extremely smooth and boron-fluorine co-doped TiO₂ nanotube arrays with enhanced photoelectrochemical and photocatalytic performance. *Electrochim Acta* 139:331–336
 32. Xing JH, Hui L, Xia ZB, Chen JQ, Zhang YH, Li Z (2014) Influence of substrate morphology on the growth and properties of TiO₂ nanotubes in HBF₄⁻ based electrolyte. *Electrochim Acta* 134:242–248
 33. Kitada A, Hasegawa G, Kobayashi Y, Kanamori K, Nakanishi K, Kageyama H (2012) Selective preparation of macroporous monoliths of conductive titanium oxides Ti_nO_{2n-1} (n = 2, 3, 4, 6). *J Am Chem Soc* 134(26):10894–10898
 34. Su HF, Wang T, Zhang SY, Song JM, Mao CJ, Niu HL, Jin BK, Wu JY, Tian YP (2012) Facile synthesis of polyaniline/TiO₂/graphene oxide composite for high performance supercapacitors. *Solid State Sci* 14(6):677–681
 35. Cai GF, Tu JP, Zhou D, Zhang JH, Xiong QQ, Zhao XY, Wang XL, Gu CD (2013) Multicolor electrochromic film based on TiO₂@polyaniline core/shell nanorod array. *J Phys Chem C* 117(31):15967–15975
 36. Salari M, Aboutalebi SH, Chidembo AT, Nevirkovets IP, Konstantinov K, Liu HK (2012) Enhancement of the electrochemical capacitance of TiO₂ nanotube arrays through controlled phase transformation of anatase to rutile. *Phys Chem Chem Phys* 14(14):4770–4779
 37. Peng X, Huo KF, Fu JJ, Zhang XM, Gao B, Chu PK (2013) Coaxial PANI/TiN/PANI nanotube arrays for high-performance supercapacitor electrodes. *Chem Commun* 49(86):10172–10174
 38. Stève B, Daniel B (2005) Electrochemical derivatization of carbon surface by reduction of in situ generated diazonium cations. *J Phys Chem B* 109:24401–24410
 39. Santos LM, Ghilane J, Fave C, Lacaze PC, Randriamahazaka H, Abrantes LM, Lacroix JC (2008) Electrografting polyaniline on carbon through the electroreduction of diazonium salts and the electrochemical polymerization of aniline. *J Phys Chem C* 112(41):16103–16109
 40. Tiddia M, Mula G, Mascia M, Sechi E, Vacca A (2016) Porous silicon–polyaniline hybrid composites synthesized through electroreduction of an aryldiazonium salt: preparation and photocurrent properties. *RSC Adv* 6(104):101880–101887
 41. Greenwood J, Phan TH, Fujita Y, Li Z, Ivashenko O, Vanderlinden W, Gorp HV, Frederickx W, Lu G, Tahara K (2015) Covalent modification of graphene and graphite using diazonium chemistry: tunable grafting and Nanomanipulation. *ACS Nano* 9(5):5520–5535
 42. Zhang QQ, Li Y, Feng YY, Feng W (2013) Electropolymerization of graphene oxide/polyaniline composite for high-performance supercapacitor. *Electrochim Acta* 90:95–100
 43. Chen JQ, Xia ZB, Li H, Li Q, Zhang YH (2015) Preparation of highly capacitive polyaniline/black TiO₂ nanotubes as supercapacitor electrode by hydrogenation and electrochemical deposition. *Electrochim Acta* 166:174–182
 44. Singu BS, Male U, Srinivasan P, Yoon KR (2017) Preparation and performance of polyaniline–multiwall carbon nanotubes–titanium dioxide ternary composite electrode material for supercapacitors. *J Ind Eng Chem* 49:82–87
 45. Mousli F, Chaouchi A, Hocine S, Lamouri A, Rei Vilar M, Kadri A, Chehimi MM (2019) Diazonium-modified TiO₂/polyaniline core/shell nanoparticles. Structural characterization, interfacial aspects and photocatalytic performances. *Appl Surf Sci* 465:1078–1095

Publisher's note Springer Nature remains neutral with regard to jurisdictional claims in published maps and institutional affiliations.